Anal. Bioanal. Electrochem., Vol. 11, No. 3, 2019, 396-406

Analytical & Bioanalytical Electrochemistry

2019 by CEE
www.abechem.com

Full Paper

Effect of Vanadium Pentoxide (V_2O_5) on the Corrosion Protection Performance of Zn-Mn-V_2O_5 Composite Coating on Mild Steel

Dyamanna Thippeswamy, Yanjerappa Arthoba Nayaka* and Matad Mallikarjunaiah Vinay

Department of Chemistry, School of Chemical Sciences, Kuvempu University, Shankaraghatta - 577451, Karnataka, India

*Corresponding Author, Tel.: +91-9448855078; Fax: +91-8282 256255

E-Mail: drarthoba@yahoo.co.in

Received: 22 August 2018 / Received in revised form: 13 January 2019 / Accepted: 17 March 2019 / Published online: 31 March 2019

Abstract- The electrodeposit of Zn-Mn-V_2O_5 alloy composite coating has been obtained on the surface of steel using acid sulphate bath. The bath composition and operating variables such as pH, current density and temperature were optimized through Hull-cell experiments. The corrosion properties of Zn, Zn-Mn and Zn-Mn-V_2O_5 have been studied in 3.5% wt. NaCl using potentiodyanamic polarization measurements like Tafel extrapolation and which showed the corrosion rates (CR) of 7.234×10^{-5} g h^{-1}, 5.392×10^{-5} g h^{-1}, and 2.909×10^{-6} g h^{-1}, respectively. The polarization resistance (R_P) values of 938.9 Ω cm^2, 3403.8 Ω cm^2 and 4287.5 Ω cm^2 by electrochemical impedance spectroscopy (EIS) also confirm the better corrosion resistance of Zn-Mn-V_2O_5 compare to Zn, Zn-Mn alloy coatings. The current efficiency and throwing power of the optimized bath solution were measured. The surface morphology of Zn-Mn-V_2O_5 composite coating has been analyzed by SEM. The X-ray diffraction analysis (XRD) was employed to study the average crystallite size of the composite coatings.

Keywords- Corrosion, EDX, EIS, Tafel, Zn- composite coating

1. INTRODUCTION

Zn-Mn-V_2O_5 alloy composite coating is an industrial process and generally employed to coat on surface of the steel (as cathode) for increase its long duration. The composite coating acquires synergistic properties of its matrix and the guest material. According to the nature of matrices, nano-composites can be classified into three main categories i.e. metal-matrix, ceramic-matrix and polymer-matrix nano composites [1].

The different methods have been considered to generate nanocomposite materials namely, thermal, plasma sparing, electrodeposition, physical and chemical vapour deposition [2]. Among these, electrodeposition method is being generally employed since it finds many improvements such as controllable experimental parameters, low energy requirements, homogeneous coating, low-cost, flexibility, increase of production rate and decrease of wastes [3,4]. The decrease in grain size of metal deposits provides to an enhancement in strength and strain properties [5]. In electrodeposition of zinc metal, the different particles have been employed such as TiO_2, SiO_2, Al_2O_3, CeO2, ZrO_2, SnO_2 and Cr_2O_3, carbides like WC, TiC, Si_3N_4 [6,7-11] and SiC, nitrides like and BN, carbon nanotubes etc. [12-15]. In particular zinc-manganese alloy composite coatings obtained by electrodeposition are characterized by their superior corrosion resistance and wear resistance [16].

The composite coating is an advanced method in material science. Another important application is the possibility to co-deposit metal with metallic, non-metallic, polymeric particles etc. The demand for newly developed materials based on composite metal matrix shows a better tendency owing to their prospective applications in many industrial zones [17-21]. The zinc and zinc-manganese alloy composite coatings can be also applied for corrosion prevention since it is well known that most of them exhibit very high corrosion resistance [22-27].

The nanoparticles of vanadium pentoxide (V_2O_5) possess the properties such as high catalytic activity, more surface area, better chemical stability and photochemical activity [28,29]. In this paper electrochemical studies of Zn-Mn-V_2O_5 composite coating on the surface of mild steel by using acid sulphate bath containing various additives has been undertaken and the performance of corrosion rate of the composite coatings were examined by employing electrochemical technique such as Tafel extrapolation and impedance measurements (EIS). The composition and surface of photomicrographs of Zn-Mn-V_2O_5 composite layer were evaluated by SEM and X-ray diffraction.

2. EXPERIMENTAL

2.1. Zn-Mn alloy composite coating

The process of electrodeposition of Zn-Mn-V_2O_5 composite coating on mild steel comprises the following sequence of steps, viz., alkaline cleaning, activation, pre-electroplating. The bath compositions and operating conditions for coating electroplating of Zn-Mn alloy were as follows: $ZnSO_4.7H_2O$ 200 gL^{-1}, Na_2SO_4 60 gL^{-1}, H_3BO_3 16 gL^{-1}, cetyl trimethyl ammonium bromide 20 gL^{-1}, pH 3.0-4.0, cathode current density 1 A/cm^2 and electroplating time 10 min.

The mild steel plates were polished mechanically and degreased by dipping in boiled trichloroethylene followed by water wash and then the plates were immersed in 10% hydrochloric acid to remove the rust and finally rinsed with water and used as cathode. The pure zinc plate [99.99%] was employed as anode and its surface was activated by immersing in 5% hydrochloric acid for 2-5 seconds followed by water wash.

2.2. Composite coating

The composite coatings are electrochemically deposited from same electroplating bath and at the same electrodeposition conditions described above but with an addition of powdered vanadium pentaoxide (V_2O_5) of 0.5 gL^{-1}. The composite coating of Zn-Mn with vanadium pentaoxide (V_2O_5) was generated on the surface of the mild steel from optimized acid sulphate bath solution using Hull cell experiments (Table 1). The performances of corrosion rate of Zn-Mn-V_2O_5 composite coatings were examined by electrochemical measurements using Tafel and EIS. All electrochemical measurements were carried out by electrochemical work station (Model number: CH Instrument 660D, USA). A three electrode convention cell comprising of platinum as counter electrode, saturated calomel as reference electrode and specimen under investigation as working electrode (1×1 cm^2) was used for Polarization and electrochemical impedance studies in 3.5% wt. NaCl solution.

3. RESULTS AND DISCUSSION

For pure zinc deposition, zinc metal with dimension 6 cm×6.5 cm and mild steel specimen of dimension 10 cm×7.5 cm were used as anode and cathode respectively. The pretreatment of cathode and anode surfaces has been done as per the procedure stated in the division of experimental. The obtained electrodeposits from optimized bath constitution and operating parameters as shown in Table 1. The standard Hull-Cell of 267 mL capacity made up of Perspex material was employed to assess and optimizing the bath constituents and operating variables for the generation of excellent deposits. A 1 A of cell current was used for 10 min. After plating experiments, the coating plates were dipped in 5% nitric acid for 2

seconds then rinsed with water [30]. The nature and manifestation of coating Zn-Mn alloy was cautiously studied and recorded through the codes of Hull-Cell as shown in Figure 1. All the electroplating experiments were conducted at 303 K.

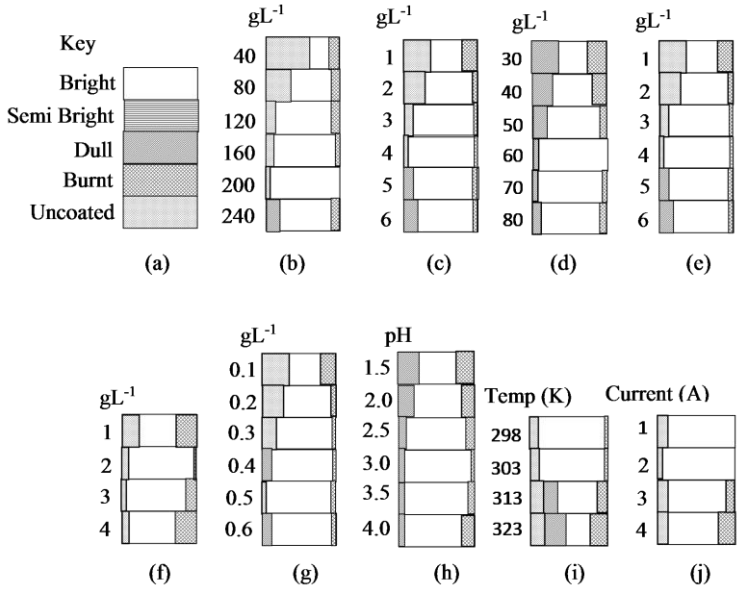

Fig. 1. Hull-cell figures: (a) Key; (b) $ZnSO_4.7H_2O$; (c) $MnSO_4.H_2O$; (d) Na_2SO_4; (e) H_3BO_3; (f) CTAB; (g) V_2O_5; (h) pH; (i) Temperature; (j) Cell current

Table 1. Optimum bath composition and operating condition

Bath composition	**Quantity gL^{-1}**	**Operating conditions**
$ZnSO_4.7H_2O$	200	Anode: Zinc metal (99.99%)
$MnSO_4.H_2O$	4	Cathode: mild steel
Na_2SO_4	60	Plating time:10 min
H_3BO_3	16	pH: 3.0
CTAB	2	Temperature: 293-303 K
V_2O_5	0.5	Cell current:1A

The optimized sulphate bath (Table 1) containing 0.5 gL^{-1} of V_2O_5 was stirred for 2 h for homogeneous distribution of V_2O_5 nanoparticles. The Hull-Cell experiments were carried out to assess and optimize the bath composition and operating conditions for the production of good quality Zn-Mn-V_2O_5 composite coatings.

3.1. Corrosion rate measurement

3.1.1. Tafel method

The polarization measurements were carried out in a three electrode cell comprising Zn-Mn-V_2O_5 composite coated specimen as working electrode, saturated calomel as reference electrode and platinum wire as counter electrode. The obtained polarization curves of pure Zn and Zn-Mn-V_2O_5 composite coating in corrosion media (3.5 wt% of NaCl solution), are shown in Figure 2. Polarization data were measured at their OCP of relevant coatings and the obtained parameters of corrosion kinetics with reference to saturated calomel electrode and are tabulated in Table 2.

The corrosion potentials (E_{corro}) of Zn-Mn-V_2O_5 composite coatings are less negative than pure Zn coating. This shows that the Zn-Mn-V_2O_5 composite coating possess an excellent corrosion inhibition property. The corrosion current density for pure Zn coating, Zn-Mn alloy coating and Zn-Mn-V_2O_5 composite coating were found to be 6.077×10^{-5}, 4.530×10^{-5}, and 2.444×10^{-6}, respectively. The coating of Zn-Mn-V_2O_5 possess lowest I_{corro} value than pure zinc coating, The lowest I_{corro} of Zn-Mn-V_2O_5 coating is attributed to the incorporation of V_2O_5 nanoparticles into the zinc matrix. The incorporation of V_2O_5 nanoparticles leads to an area of active surface is decrease or anodic sites in Zn-Mn alloy coating. The presence of V_2O_5 nanoparticles in Zn-Mn alloy matrix improved the properties such as corrosion resistance and wear resistance of Zn-Mn alloy deposited steel due to the presence of nanoparticles of V_2O_5, which generate new nucleation sites compare to Zn-Mn alloy and decrease the grain size of the deposit and hence results in the formation of new homogeneous passive surface.

The anodic and cathodic Tafel slope values of Zn-Mn-V_2O_5 alloy composite coatings are distinct from plain zinc coating.

Table 2. Corrosion parameters of the coating estimated from Tafel plots

Specimen	**E_{corro} V**	**I_{corro} Acm^{-2}**	**β_c**	**β_a**	**Lp Ω cm^2**	**CR g h^{-1}**
Zn	-1.120	6.077×10^{-5}	7.650	16.305	390	7.234×10^{-5}
Zn-Mn	-1.101	4.530×10^{-5}	6.400	24.049	2302	5.392×10^{-5}
Zn-Mn-V_2O_5	-1.024	2.444×10^{-6}	5.020	30.256	4120	2.909×10^{-6}

This indicates the influence of V_2O_5 nanoparticles on the kinetics of both cathode and anodic reaction of zinc-coating and also improved anticorrosion property of composite coating as it was confirmed by E_{corro} and I_{corro} data. Major corrosion parameters, corrosion current density(I_{corro}), corrosion potential (E_{corro}), Tafel slopes (β_c and β_a), linear polarization (Lp) and corrosion rate were calculated by extrapolating the linear section of the Tafel plots following equation and presented in Table 2.

$$CR = \frac{0.13 \times I_{corro} \times Eq.Wt.of\ Zn}{d}$$

Where d=density of Zn

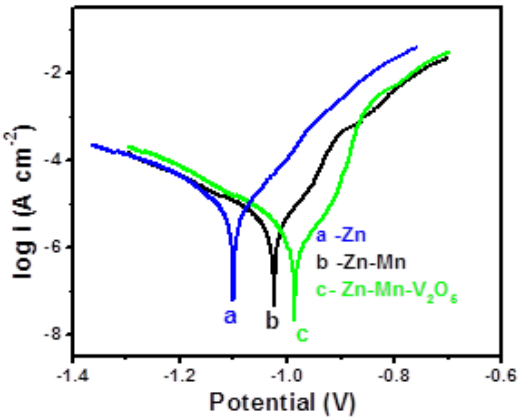

Fig. 2. Polarization curves for zinc and Zn-Mn-V_2O_5 composite coatings in 3.5% wt. NaCl solution

3.1.2. Electrochemical Impedance Studies

The EIS measurement is useful method to evaluate the performance of corrosion rate of the composite coating on metal surface [31,32]. The corrosion resistance property of zinc and Zn-Mn-V_2O_5 composite deposits were examined by electrochemical impedance method in 3.5 wt% NaCl solution at the frequency between 0.1 Hz to 100 kHz are shown in Figure 3(A). The measurements of impedance were carried out at their open circuit potential for the resultant coatings. Nyquist plots were exhibited as imaginary impedance component (Z″) *vs.* real impedance component (Z′). The Figure 3(B) presents the EIS results which were analyzed in terms of equivalent circuit model and illustrate the corrosion parameters of the composite coatings. In this model R_s is the resistance of coating, R_{ct} is resistance of charge transfer, Q_{coat} is capacitance of coating and Q_{dl} is the capacitance of the double layer. The constant phase element (CPE) indicate or denote that the behavior of non-ideal capacitance of the working electrode owing to homogeneous of the surface. The impedance is given by the following equation:

$$\mathbf{Z_{CPE} = Y_0^{-1}(i\omega)^{-n}}$$

Where Y_0 is the constant phase element (CPE), i^2 =-1, an imaginary number, ω is angular frequency and n is exponent of CPE used to denote the micro roughness, porosity and inhomogeneity of the metal surface.

The R_{coat} and Q_{coat} denote the resistance of coating and capacitance of coating of the working electrode. The value of R_{coat} is found to be increased for Zn-Mn-V_2O_5 composite coating owing to lesser pores on the cathode surface than plain zinc coated plate. The enhanced porosity on the surface of coating allows the electrolyte solution to join with coated material and the possibility of corrosion product formation increases. The Q_{dl} denotes double layer capacitance of electrode and electrolytic solution. The lesser Q_{dl} value of Zn-Mn-V_2O_5 alloy composite coating shows that the stability of coated surface is increased towards corrosive environment compare to Zinc and Zinc-Manganese alloy deposition. The value of R_{ct} is related to the redox process take place at electrode surface owing to corrosion product is generated. The lower R_{ct} value signifies the generation of a thin layer corrosion product on surface of the working electrode. The analyzed impedance data were presented in **Table 3.** The resistance of polarization was calculated by the addition of R_{coat} and R_{ct}. The R_p value is found to greater for Zn-Mn-V_2O_5 composite coating than Zn-Mn alloy and zinc depositions. From polarization studies and Nyquist plot analysis, illustrated that Zn-Mn-V_2O_5 composite coating exhibits better corrosion resistance than Zn-Mn alloy and Zinc depositions.

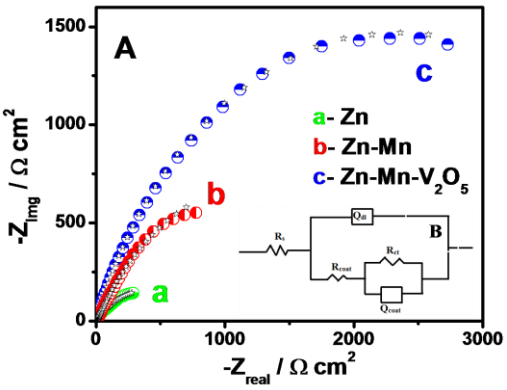

Fig. 3. (A) Nyquist plot of: (a) Zn; (b) Zn-Mn alloy; (c) Zn-Mn-V_2O_5 composite coating; **(B)** Equivalent circuit model for Zn-Mn-V_2O_5 composite coating

Table 3. Results of Electrochemical impedance studies

Specimen	**R_{coat} Ω cm^2**	**R_{ct} Ω cm^2**	**Q_{coat} Ω cm^2**	**Q_{dl} Ω cm^2**	**n**	**$R_p = R_{coat} + R_{ct}$ Ω cm^2**
Zn	934.5	4.484	1×10^{-3}	9.349×10^{-1}	1	938.9
Zn-Mn	3393	10.87	7.4×10^{-5}	3.401×10^{-2}	1	3403.8
Zn-Mn-V_2O_5	3988	299.50	4.2×10^{-5}	3.993×10^{-3}	1	4287.5

3.2. Current Efficiency and Throwing Power

Current efficiency and throwing power were studied at various current densities by employing optimum acid bath solution. At lesser current density (1 A dm^{-2}) the current efficiency was find out 57%. At 2 A dm^{-2} current density, the current efficiency was enhanced up to 59%. The highest current efficiency of 65% was determined at 4 A dm^{-2}. With increase in current density more than 4 A dm^{-2} the current efficiency was found to be reduced. Throwing power was measured by using Haring and Blum cell at various current densities. At lesser a current density the throwing power was 19% and with enhances in the current density was increased to 28% is tabulated in a Table 4.

Table 4. Current density and Throwing power at different current densities

Current Density (A dm^{-2})	Current Efficiency (%)	Throwing Power (%)
1	57	18
2	59	22
3	63	24
4	65	28
5	53	23

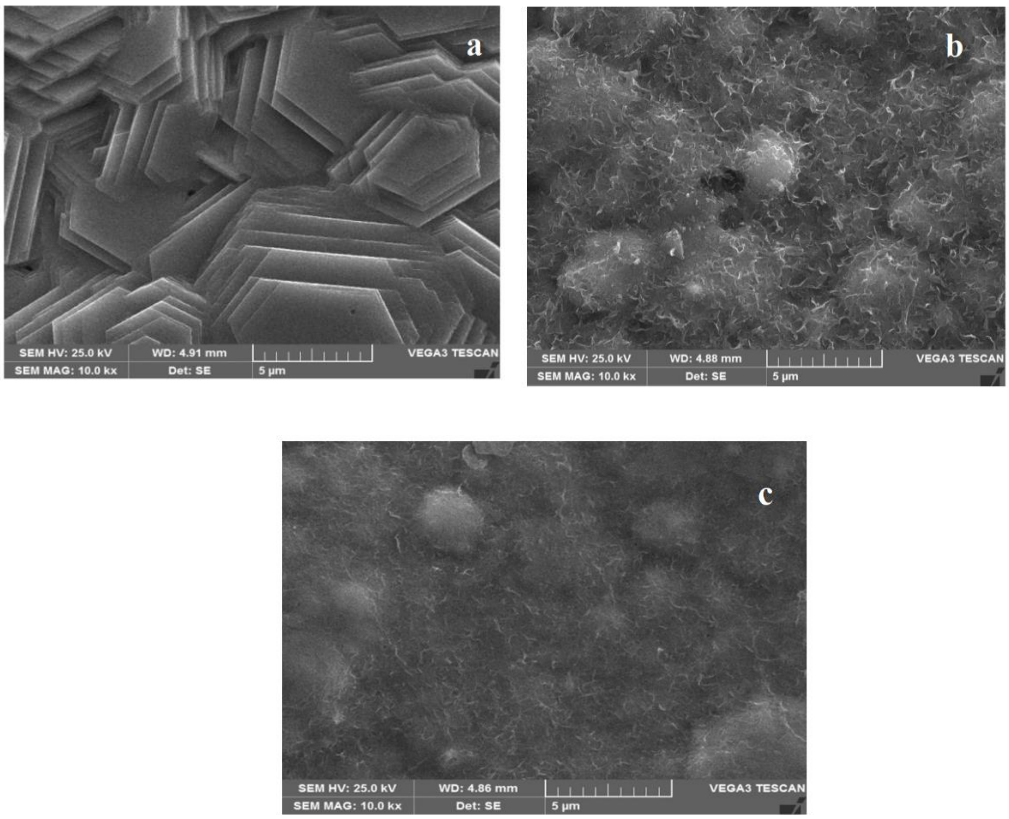

Fig. 4. SEM images of (a) Zn coating (b) Zn-Mn alloy coating (c) Zn-Mn-V_2O_5 composite coating

3.3. Surface morphology

Figure 4 shows microstructure images of Zn, Zn-Mn alloy and Zn-Mn-V_2O_5 composite coated samples, respectively. Figure 4(a) shows the surface morphology of pure zinc deposit obtained without V_2O_5 nanoparticles and it revealed the presence of irregular hexagonal shaped morphology. Figure 4(b) indicates the surface morphology of Zn-Mn alloy coating obtained with V_2O_5 nanoparticles, which shows smaller grain size of alloy deposit and created more nucleation sites for Zn-Mn alloy deposit, reduces the crystal size and thus responsible for the formation of homogeneous surface structure than plain zinc coating [33].

During electrodeposition, V_2O_5 nanoparticle distribute homogeneously in the composite coating and thus initiates new nucleation sites for further deposition, hence retards the development of crystals Figure 4(c).

3.4. XRD Studies

The XRD profile obtained for pure zinc and Zn-Mn-V_2O_5 composite coatings is present in Figure 5.

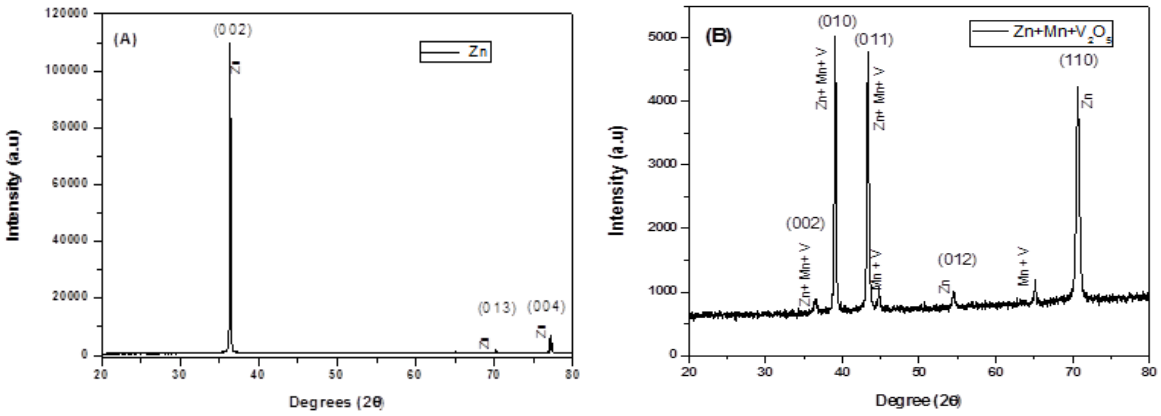

Fig. 5. XRD patterns of (A) Zn coating; (B) Zn-Mn-V_2O_5 composite coating

Average crystal size for pure zinc and Zn-Mn-V_2O_5 composite coatings were calculated from the Debye-Scherer's formula and found to be 49.65 nm and 25.67 nm, respectively. Inclusion of V_2O_5 nanoparticles into the Zn-Mn alloy plating decreases the grain size, due to the following factors; a) incorporation of V_2O_5 nanoparticles into the budding matrix gives more surface area for various nucleations and b) the V_2O_5 nanoparticles enhance the deposition potential by overfilling the strong cathode surface area, which provides to a finer grained size [34] and the Scherer's equation is given by:

$$D=K\lambda/\beta\cos\theta$$

Where, D is the diameter of the crystal K is the Scherer constant (0.9); λ is the wavelength of radiation source used, β is the angular peak with Full Width Half Maximum (FWHM) intensity and θ is the Bragg s angle.

4. CONCLUSION

The zinc, zinc-manganese alloy and zinc-manganese-vanadium pentoxide composite coatings were generated on the surface of mild steel by using acid sulphate bath. The measured CR values of 7.234×10^{-5} g h^{-1}, 5.392×10^{-5} g h^{-1}, and 2.909×10^{-6} g h^{-1} by Tafel extrapolation and R_P values of 938.9 Ω cm^2, 3403.8 Ω cm^2 and 4287.5 Ω cm^2 by EIS clearly indicated the excellent wear resistance and corrosion resistance property of Zn-Mn-V_2O_5 compare to Zn, Zn-Mn alloy coatings. The composite coating was found graphic structure and smaller in crystal size of deposits were estimated from SEM and XRD studies. Hence Zn-Mn-V_2O_5 composite coating can be used for industrial applications where high corrosion resistance is required.

REFERENCES

[1] Y. X. Gan, Micron 43 (2012) 782.
[2] D. K. Singh, and V. B. Singh, Mater. Sci. Eng. A 532 (2012) 493.
[3] J. L. Stojak, J. Fransaer, J. B Talbot, and R. C. Alkire, D. M. Kolb (Eds.), Wiley-VCH verlag, Weinheim (2002).
[4] R. K. Saha, and T. I. Khan, Surf. Coat. Technol. 205 (2010) 890.
[5] T. Lampke, B. Wielage, D. Dietrich, and A. Leopold, Appl. Surf. Sci. 253 (2006) 2399.
[6] K. Kumar, R. Chandramohan, and D. Kalyanaraman, Appl. Surf. Sci. 277 (2004) 383.
[7] M. Stroumbouli, P. Gyftou, E. A. Pavlatou, and N. Spyrellis, Surf. Coat. Technol. 195 (2005) 325.
[8] S. C. Wang, and W. C. J. Wei. Mater. Chem. Phys. 78 (2003) 574.
[9] P. Nowak, R. P. Socha, M. Kaisheva, J. Franasaer, J. P. Celis, and Z. Stoinov, J. Appl. Eletrochem. 30 (2000) 429.
[10] G. Maurin, and A. Lavannt, J. Appl. Elctrochem. 25 (1995) 1113.
[11] P. Gyftou, E. A. Pavlatou, N. Spyrellis, and K. S. Hatzilyberis, Trans. Inst. Met. Finish. 78 (2000) 223.
[12] P. Gyftou, M. Stroumbouli, E. A. Pavlatou, and N. Spyrellis, Trans. Inst. Met. Finish. 80 (2002) 88.
[13] M. A. Khazrayie, and A. R. S. Aghdam, Trans. Nonferrous. Met. Soc. China 20 (2010) 1017.
[14] C. M. P. Kumar, and T. V. Venkatesha, Phys. Scr. 86 (2012) 015804.

[15] E. Pompei, L. Magagnin, N. Lecis, and P. L. Cavallotti, Electrochem. Acta 54 (2009) 2571.
[16] S. Shivakumara, and Y. A. Naik, Bull. Mater. Sci. 30 (2007) 1-8.
[17] A. Grosjean, M. Rezrazi, J. Takadoum, and P. Bercot, surf. Coat. Technol. 137 (2001) 92.
[18] P. A. Gay, P. Bercot, and J. Pagetti, Surf. Coat. Technol. 140 (2010) 147.
[19] A. F. Zimmerman, G. Palumbo, K. T. Aust, and U. Erb, Matter. Sci. Eng. A 328 (2002) 137.
[20] K. H. Hou, M. D. Ger, L. M. Wang, and S. T. Ke, Wear. 253 (2002) 994.
[21] L. Shi, C. F. Sun, F. Zhou, and W. M. Liu, Mater. Sci. Eng. A 397 (2005) 190.
[22] E. V. Skorb, D. Fix, D. V. Andreeva, H. Mohwald, and D. Shchukin, Adv. Funct. Mater. 19 (2009) 2373.
[23] M. L. Zheludkevich, D. G. Shchnkin, K. A. Yasakan, H. Mohwald, and M. G. S. Ferreira, Chem. Mater. 19 (2007) 402.
[24] D. G. Shchnkin, and H. Mohwald, Small. 3 (2007) 926.
[25] G. Paliwada-porebska, M. Stratmann, M. Rohwerder, K. Potje-Kamloth, Y. Lu, A. Z. Pitch, and H. Alder, Corro. Sci. 47 (2005) 3216.
[26] M. Rohwerder, S. Isik-Uppenkamp, and C. Amarnath, Eletrochem. Acta 56 (2001) 1889.
[27] V. Amendola, and M. Meneghetti, Nano. scale. 19 (2009) 74.
[28] L. W. Miller, M. I. T. Tejedor, and M. A. Anderson, Environ. Sci. Technol. 33 (1999) 2070.
[29] A. L. Linsebigler, G. Lu, and J. T Yates, J. Chem. Rev. 95 (1995) 735.
[30] Y. A Naik, T. V. Venkatesh, and P. V. Nayak, Indian J. Chem. Technol. (2001) 390.
[31] M. Mahdavian, and M. M. Attar, Electrochim. Acta 50 (2005) 4645.
[32] R. Berlia, M. K. P. Kumar, and C. Srivastava, RSC Adv. 5 (2015) 71413.
[33] Y. A. Naik, T. V. Venkatesh, and P. V. Nayak, Bull. Mater. Sci. 16 (2000) 481.
[34] Y. A. Naik, and T. V. Venkatesh, Bull. Mater. Sci. 28 (2005) 495.